A role for a novel centrosome cycle in asymmetric cell division

Nasser M. Rusan[1] and Mark Peifer[1,2]

[1]Department of Biology and [2]Lineberger Comprehensive Cancer Center, University of North Carolina at Chapel Hill, Chapel Hill, NC 27599

Tissue stem cells play a key role in tissue maintenance. *Drosophila melanogaster* central brain neuroblasts are excellent models for stem cell asymmetric division. Earlier work showed that their mitotic spindle orientation is established before spindle formation. We investigated the mechanism by which this occurs, revealing a novel centrosome cycle. In interphase, the two centrioles separate, but only one is active, retaining pericentriolar material and forming a "dominant centrosome." This centrosome acts as a microtubule organizing center (MTOC) and remains stationary, forming one pole of the future spindle. The second centriole is inactive and moves to the opposite side of the cell before being activated as a centrosome/MTOC. This is accompanied by asymmetric localization of Polo kinase, a key centrosome regulator. Disruption of centrosomes disrupts the high fidelity of asymmetric division. We propose a two-step mechanism to ensure faithful spindle positioning: the novel centrosome cycle produces a single interphase MTOC, coarsely aligning the spindle, and spindle–cortex interactions refine this alignment.

Introduction

Centrosomes are critical microtubule (MT) nucleators and organizers in animal cells (Alberts et al., 2002). Centrioles form the centrosome core and are surrounded by pericentriolar material (PCM) containing MT nucleating factors like γ-tubulin (γtub; Delattre and Gonczy, 2004). Centrosomes play key roles in many processes, including organizing mitotic spindle poles (Kellogg et al., 1994).

In animal cells, centrosome duplication occurs by a conserved cycle (Alberts et al., 2002). It begins with centriole disengagement in late mitosis (Kuriyama and Borisy, 1981), followed by procentriole assembly along the wall of each centriole in S phase. By G2, cells contain two mother/daughter centriole pairs that remain in proximity until mitosis. Both centriole pairs form functional centrosomes, maturing synchronously before mitotic entry, by recruiting PCM and acting as MT organizing centers (MTOCs; in contrast, there is a 10-min delay in activating the second yeast MTOC; Shaw et al., 1997). The centrosomes then move to opposite sides of the nucleus to organize spindle poles and asters that position the spindle with respect to cortical cues. The essential role of centrosomes in animal cells was called into question by the fact that flies lacking functional centrosomes, or lacking centrioles entirely, live to adulthood (Megraw et al., 2001; Basto et al., 2006). However, not all is well: these animals have defects in divisions of larval neural stem/progenitor cells, the central brain neuroblasts (NBs).

Adult tissue stem cells play key roles in tissue maintenance/repair (Nystul and Spradling, 2006). In each division, the daughters differ in fate: one retains stem cell character and the other differentiates. *Drosophila melanogaster* central brain NBs are a superb model for asymmetric divisions of postembryonic tissue stem cells (Savoian and Rieder, 2002; Siller et al., 2005). Both embryonic and larval NBs are polarized cells exhibiting strict division patterns crucial for their roles as stem cells. Unlike the precise relationship between the embryonic NB division axis and adjacent epithelium, larval central brain NBs (Fig. 1 A) do not appear to divide with specific orientations relative to the brain as a whole (Fig. 1 B). However, each NB creates a simpler microenvironment (Fig. 1 C): the NB and its ganglion mother cell (GMC) daughters. NBs divide asymmetrically, and the NB daughter retains stem cell character, whereas the GMC daughter goes on to differentiate. NBs divide according to strict local rules; each GMC is born adjacent to the previous GMC (Fig. 1 E and Video 1, available at http://www.jcb.org/cgi/content/full/jcb.200612140/DC1; Akong et al., 2002), creating a GMC cap on one side of the NB (Fig. 1, C and D).

Correspondence to Mark Peifer: peifer@unc.edu

Abbreviations used in this paper: GMC, ganglion mother cell; MT, microtubule; MTOC, MT organizing center; NB, neuroblast; NEB, nuclear envelope breakdown; PCM, pericentriolar material.

The online version of this article contains supplemental material.

The Journal of Cell Biology, Vol. 177, No. 1, April 9, 2007 13–20
http://www.jcb.org/cgi/doi/10.1083/jcb.200612140

Although differential fate allocation is critical in stem cells, we have much to learn about how a stereotyped division axis is established. NBs must coordinate cortical and spindle polarity so that neural determinants are packaged into the differentiating daughter (Yu et al., 2006). Mutations affecting polarity or astral MT cortical interactions result in asymmetric division defects (Yu et al., 2006). The importance of a properly aligned spindle is also suggested by spindle alignment defects in the absence of centrioles (14% symmetric divisions; Basto et al., 2006) or in mutants that lack PCM (*asterless* [*asl*] or *centrosomin* [*cnn*]) and have few or no astral MTs (Giansanti et al., 2001; Megraw et al., 2001). Thus, proper interactions between the spindle, astral MTs, and cortical polarity cues help maintain a constant division axis. Previous analyses revealed that NB spindles form at prophase already roughly aligned with the ultimate division axis (Siller et al., 2006) but did not define how the initial axis forms.

Here, we address how this model stem cell maintains a persistent division axis. *D. melanogaster* male germline stem cells also have a persistent division axis. It was proposed that one centrosome is cortically anchored by MT–adherens junction interactions (Yamashita et al., 2003). To test whether a similar mechanism exists in NBs, we analyzed the centrosome cycle using 4D or 5D spinning disk confocal microscopy on brains prepared with no physical distortion (Fig. S1 A, available at http://www.jcb.org/cgi/content/full/jcb.200612140/DC1), maintaining NB shape to replicate normal mitosis.

Results and discussion

NBs generate a second active MTOC during mitotic entry

By prophase, NBs contain two MTOCs that are almost fully separated and aligned along the NB/GMC axis (Siller et al., 2006), but analysis of fixed NBs revealed a single MTOC positioned opposite the GMCs before mitotic entry (Ceron et al., 2001). We thus examined MTOC behavior throughout the cell

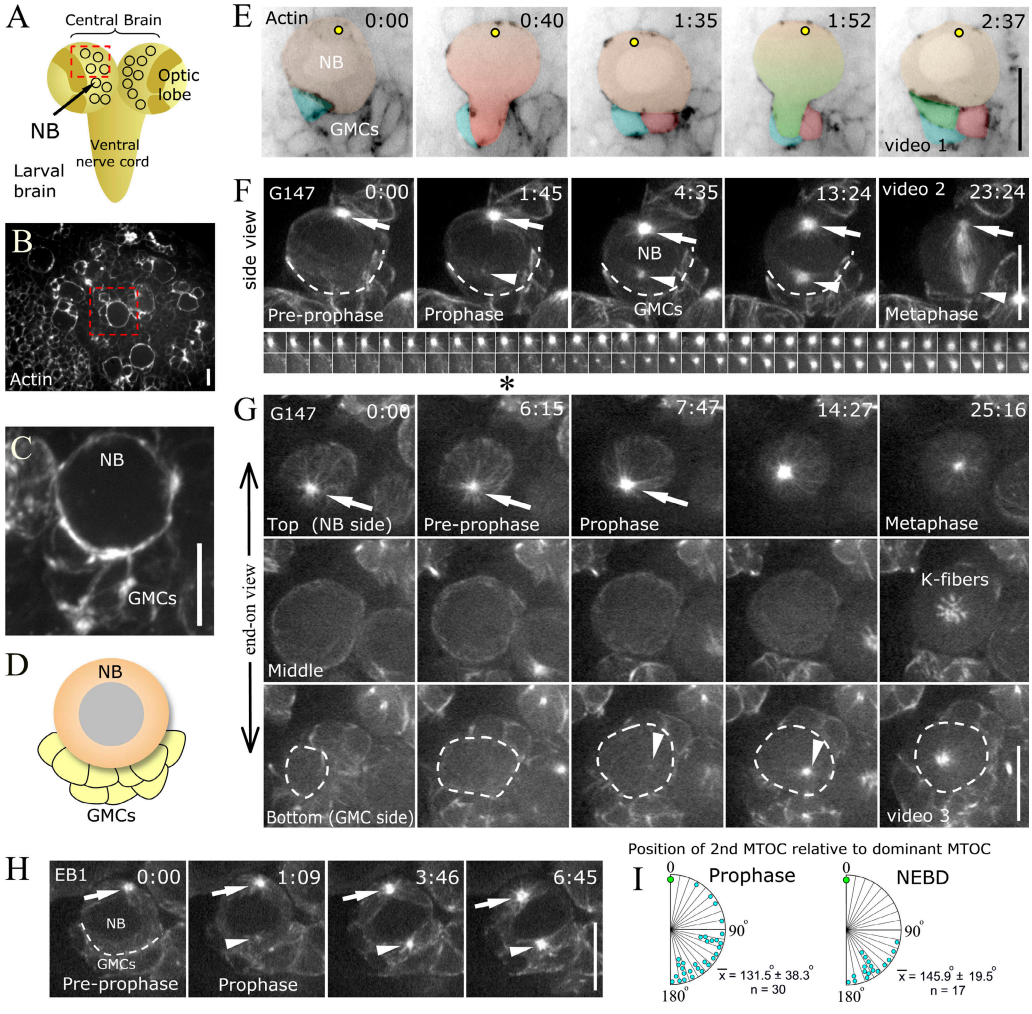

Figure 1. **NB MTOCs form asynchronously.** (A) Cartoon. (B–E) NB/GMCs in central brain (B), close-up (C and E), and cartoon (D). (B and C) Phalloidin. (E) Actin-GFP for two cell cycles; positions of successive GMCs are indicated (colored). The yellow dot represents a hypothetical MTOC. (F and G) GFP-G147 NBs. (F) GMCs are indicated by the dotted line. Max-intensity projections are shown for entire cell. Single MTOC matures and forms MT basket (0:00; arrow). Second MTOC appears on other side of nucleus (1:45; arrowhead) and matures (4:35). Small images show dominant MTOC (top) and second MTOC (bottom; asterisk). (G) An end-on view of MTOC maturation, three sections of z stack. Dominant MTOC is present throughout (top, arrows). Second MTOC appears (7:74; arrow). Dotted line indicates bottom of NB. (H) EB1-GFP. Second nucleation center appears (1:09; arrow). (I) Position where second MTOC appears relative to dominant MTOC. Time is shown as h:min (E) and min:s (F–H). Bars, 10 µm.

cycle as an initial approach to test the hypothesis that fixing the position of one MTOC through successive divisions helps ensure persistent spindle orientation. We analyzed live NBs expressing GFP-G147, an MT-associated protein (Morin et al., 2001), revealing a striking temporal difference in MTOC activity. During interphase, a single detectable MTOC persists opposite the previous division site; we refer to this as the dominant MTOC. As NBs approach mitosis, this MTOC increases activity (matures; empirically judged by size and MT fluorescence intensity), forming an MT basket around the nucleus (Fig. 1, F and G, 0:00, arrows; and Videos 2 and 3, available at http://www.jcb.org/cgi/content/full/jcb.200612140/DC1). We refer to this as preprophase; this stage is also seen in fixed samples stained for tubulin (Fig. S1 B). Soon after, sometime before the dominant MTOC fully matures, something striking happens: a second MTOC appears distant from the first (Fig. 1 F, 1:45, arrowheads; and Video 2). We refer to this as the second MTOC and this stage as prophase onset. The second MTOC increases activity, maturing ~10 min before nuclear envelope breakdown (NEB; Fig. 1 F, 1:45–13:24). Using 4D imaging, we excluded the possibility that the second MTOC was present earlier in another focal plane. To further assess this, we imaged forming spindles end on (Fig. 1 G and Video 3). It is clear that the second MTOC did not emerge from the dominant MTOC (Fig. 1 G, top) or travel around the nucleus (Fig. 1 G, middle). Instead, the second MTOC appeared roughly opposite the dominant MTOC (Fig. 1 G, bottom, arrowheads; 132 ± 38° from the dominant one, using the centroid of the nucleus as a fixed reference; $n = 30$; Fig. 1 I, prophase). MTOC separation began immediately, and by NEB, they were 146 ± 20° apart ($n = 18$, Fig. 1 I; this is slightly less than seen by Siller et al., 2005 [171°], likely because of different measurement methods). Thus, NBs form two distinct MTOCs: an MTOC persisting from the previous division and another only activated at mitotic entry.

A novel centrosome cycle in NBs

This distant activation of the second MTOC raised questions about the centrosome cycle. One possibility is that NBs have two MT nucleating centrosomes, but only one can retain MTs and act as an MTOC during interphase, whereas the second acquires MT retention ability during mitotic entry, explaining the second MTOC's sudden appearance. There is precedent for this: mouse L929 cells have two γtub-bearing centrosomes that can nucleate MTs, but only one contains Ninein and can retain MTs to form an MTOC (Piel et al., 2000).

To test this hypothesis in NBs, we used EB1-GFP. This binds growing MT plus ends and reliably identifies MT nucleation sites (Mimori-Kiyosue et al., 2000; Piehl et al., 2004). Only one nucleation site was present in interphase and preprophase (Fig. 1 H, arrows; 0:00; z series not depicted), and a new nucleation site appeared distant from the first (Fig. 1 H, arrowheads), consistent with spatially and temporally distinct second MTOC activation. Thus, NBs regulate MT nucleation and not just MT retention.

To examine how the new nucleation center forms, we imaged centrosomes using a PCM protein, GFP-Cnn (Megraw et al., 2002). NBs contain a single detectable centrosome during interphase (Fig. 2 A, 0:51–2:36). When NBs reenter mitosis, a second Cnn-positive centrosome appears distant from the first (Fig. 2 A, 2:36, blue arrow), mimicking activation of the second MTOC. To verify that these occur simultaneously, we imaged NBs expressing mCherry-Tubulin (chTub) and GFP-Cnn (Fig. 2 B and Fig. S2 B, available at http://www.jcb.org/cgi/content/full/jcb.200612140/DC1). This revealed perfect temporal and spatial correlation between the appearance of the second centrosome and activation of the second MTOC (Fig. 2 B, arrowheads). We never saw physical separation of two centrosomes/MTOCs ($n > 60$). To our knowledge, this is the first example of asynchronous and physically distant centrosome maturation, suggesting that NBs use a novel centrosome cycle.

Higher temporal/spatial resolution imaging revealed that two GFP-Cnn spots separate during mitotic exit (Fig. 2 B, inset; and Video 5, available at http://www.jcb.org/cgi/content/full/jcb.200612140/DC1). One GFP-Cnn spot persists as the NB interphase centrosome, forming the dominant MTOC, whereas the other spot disappears. The persistent Cnn spot (centrosome) remains relatively stationary in interphase (see The dominant centrosome predicts spindle alignment), consistent

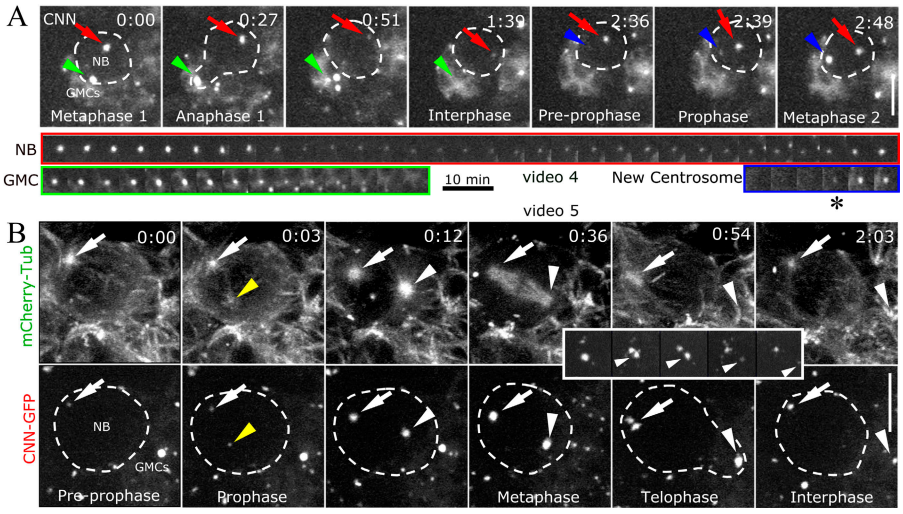

Figure 2. **Differential maturation of NB centrosomes.** (A) GFP-Cnn for one cell cycle. Dominant centrosome is indicated by the red arrows. PCM is reduced during mitotic exit and accumulates in preprophase. GMC centrosome completely loses PCM (green arrowheads). Second centrosome appears distant from dominant centrosome (blue arrowheads). The asterisk highlights the appearance of the second centrosome. (B) GFP-Cnn, chTub. Arrows indicate dominant centrosome. Arrowheads indicate second centrosome. The inset shows GFP-Cnn, PCM splitting. Time is shown as h:min. Bars, 10 μm.

with the hypothesis that coarse spindle alignment begins in interphase by anchoring the dominant centrosome (Fig. 2 A, 0:00–2:48, red arrows).

The NB daughter cells differ in PCM retention

We also examined centrosome fate in the two daughters (new NB and GMC). They differ dramatically in PCM retention, in contrast to mammalian cells, where both daughters' centrosomes retain PCM. The GMC centrosome sheds all PCM (Fig. 2 A, 0:27–0:51, green arrowheads; centrioles remain [see Asymmetric centrosome regulation]; GMCs regain PCM when reentering mitosis, Ceron et al., 2001). The new NB centrosome (that becomes the dominant MTOC) retains PCM throughout interphase (Fig. 2 A, 0:27–0:51, red arrows) and further accumulates PCM during the next mitosis (Fig. 2 A, 1:39–2:36, red arrows and Fig. S2 A). The complete shedding of PCM in GMCs appears to be the normal behavior of interphase centrosomes in most fly cells (Cottam et al., 2006; Rogers, G., personal communication), whereas in syncytial early embryos, both daughters retain PCM foci through the cell cycle. In contrast to both cell types, the NB daughters exhibit differential PCM retention.

Our data suggest that NBs have a novel centrosome cycle in which the second centrosome matures distant from the dominant centrosome/MTOC. One hypothesis to explain this would be the distal positioning of a differentially regulated centriole that is blocked from recruiting PCM in interphase and thus cannot form an MTOC until "activated" during mitosis. If this centriole is always inherited by the GMC, it might also explain complete PCM loss as GMCs exit mitosis.

Differential centriole movement

We examined centrioles live to test this hypothesis, using the centriole marker GFP-PACT (Martinez-Campos et al., 2004) and Histone-GFP (Fig. 3 A). Mother/daughter centrioles disengaged in late telophase (Fig. 3 A, 0:24; and Fig. S1 C), as in mammalian cells and fly embryos (Kuriyama and Borisy, 1981; Piel et al., 2000). Thus, two NB centrioles are present throughout interphase despite the presence of only one MTOC.

The two centrioles then exhibit different behaviors. One remains fairly stationary (Fig. 3 A, arrows), whereas the second moves to roughly the other side of the nucleus (arrowheads). Disengagement perfectly correlates with separation of Cnn spots (Fig. 2 B), suggesting that the stationary centriole retains PCM to form the dominant MTOC and the mobile centriole completely sheds PCM. To test this, we imaged NBs expressing chTub and GFP-PACT (Fig. 3 B and Video 6, available at http://www.jcb.org/cgi/content/full/jcb.200612140/DC1). The stationary centriole retained MTs (Fig. 3 B, arrows), whereas the mobile centriole did not (arrowheads). Upon reentering mitosis, the mobile centriole regained nucleation activity, forming the second MTOC.

This suggests that full separation of the MTOCs that organize the spindle is biphasic. It begins in interphase, when

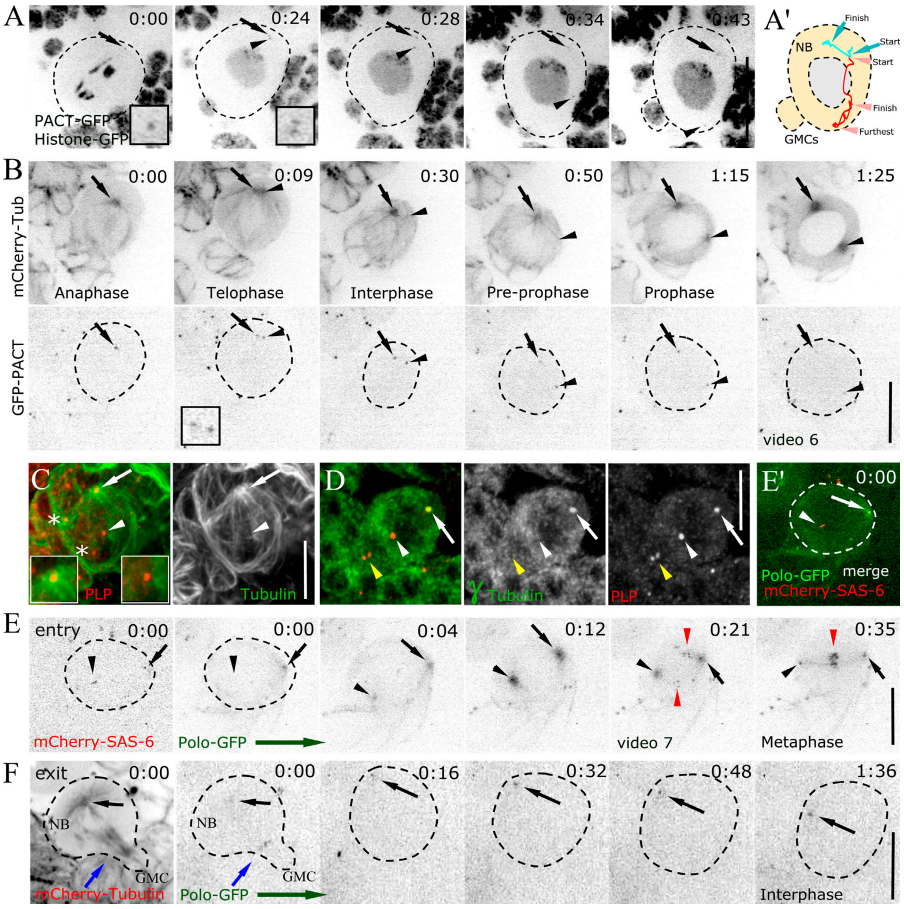

Figure 3. **NB centrioles differ in behavior and regulation.** NBs are outlined in A, B, E, and F. Imaged proteins are indicated on each figure. Images are displayed in inverse contrast. (A) Centrioles separate (each indicated by an arrow or arrowhead; 0:24; insets highlight the separation). One is relatively stationary (arrows), and the second moves to other side of nucleus (arrowheads). (A') The diagram shows the path of centrioles in A. (B) Centrioles split in late telophase; one remains stationary with associated MTs (arrows), and the other loses MTs and moves around the nucleus (arrowheads). (C and D) Fixed NBs. DPLP and MTs (C) or γtub (D) are shown. (C) Preprophase NB. One centriole is at the center of MT aster (arrows), and the other has no associated MTs (arrowheads). Asterisks show centrioles in adjacent cells that appear to be in NB by max-intensity projection. (D) Only the centriole distant from GMC cap has γtub (arrows). GMC centrioles lack γtub (yellow arrowheads). (E and E') Mitotic entry: preprophase dominant centriole has Polo (arrows), and the second does not (arrowheads). (0:04) Prophase; second centriole begins to acquire Polo (arrowheads). After NEB, Polo moves to kinetochores (0:21–0:35; red arrowheads). (F) Mitotic exit: NB retains Polo on dominant centriole from telophase into interphase (0:00–1:36; black arrows). Polo is also at midbody in telophase (blue arrows). Time is shown as h:min. Bars, 10 μm.

one centriole retains PCM, remains stationary, and forms the dominant MTOC, whereas the second centriole sheds PCM and becomes mobile. Movement of the second centriole away from the dominant MTOC in interphase accounts for ∼70% (132/180°; Fig. 1 I) of the separation needed to form a spindle. Mechanisms of transporting the mobile centriole remain to be identified, but it is nonrandom, as in 26/30 NBs, the second MTOC emerged ≥90° from the dominant MTOC (Fig. 1 I). After the second MTOC is activated, the two separate the last 30%, most likely via MT sliding forces. This might explain defects in *lissencephaly1* mutants, where MTOCs are only separated by 124° at NEB (Siller et al., 2005). Perhaps interphase centriole movement is normal, but MT-based MTOC separation is defective.

Asymmetric centrosome regulation

These data suggest that NBs differentially regulate the activity of their two centrioles within the same cytoplasm. Interestingly, a similar observation was made in clam eggs, which have three centrosomes just after fertilization. The sperm centrosome is functionally inactivated, whereas female centrosomes organize the meiotic spindle (Wu and Palazzo, 1999).

We next examined NB centrosome regulation. In prophase, one centriole (marked by anti-DPLP; Fig. S1 C) formed the dominant MTOC (Fig. 3 C, arrows), whereas the second centriole had no associated MTs and was randomly positioned (Fig. 3 C, arrowheads), confirming our live-cell data. We thus examined whether γtub is recruited asymmetrically. Fixed prophase NBs had two centrioles; only that opposite the GMCs accumulated γtub (Fig. 3 D; neither GMC centriole carried γtub [yellow arrowheads], consistent with complete Cnn loss in interphase GMCs). Further, both γtub and Cnn are absent from the NB centriole nearest the GMCs in interphase/prophase (Fig. S2 C).

Polo kinase promotes centrosome maturation by promoting γtub recruitment during mitotic entry (Glover, 2005). Differences in Polo localization/activity might underlie differences in timing of NB centrosome maturation. We examined NBs expressing Polo-GFP and the centriole marker mCherry-DSAS-6 (Dammermann et al., 2004). Only the centriole pair that forms the dominant centrosome was Polo-GFP positive during prophase (Fig. 3 E, arrows). Polo-GFP accumulated on the mobile centriole pair as the NB entered mitosis (Fig. 3, E and E′, arrowheads; and Video 7, available at http://www.jcb.org/cgi/content/full/jcb.200612140/DC1), increased on both centriole pairs through prophase, and moved on to kinetochores (Moutinho-Santos et al., 1999). When we imaged Polo-GFP in cells exiting mitosis, we could see it retained at low levels on the dominant centrosome (Fig. 3 F and Fig. S2, D–G). In the future, it will be interesting to examine the localization of Aurora A, another centrosome regulator.

Unlike the distal appendages of mammalian mother centrioles, fly mother and daughter centrioles have no known ultrastructural (Callaini and Riparbelli, 1990) or molecular differences.

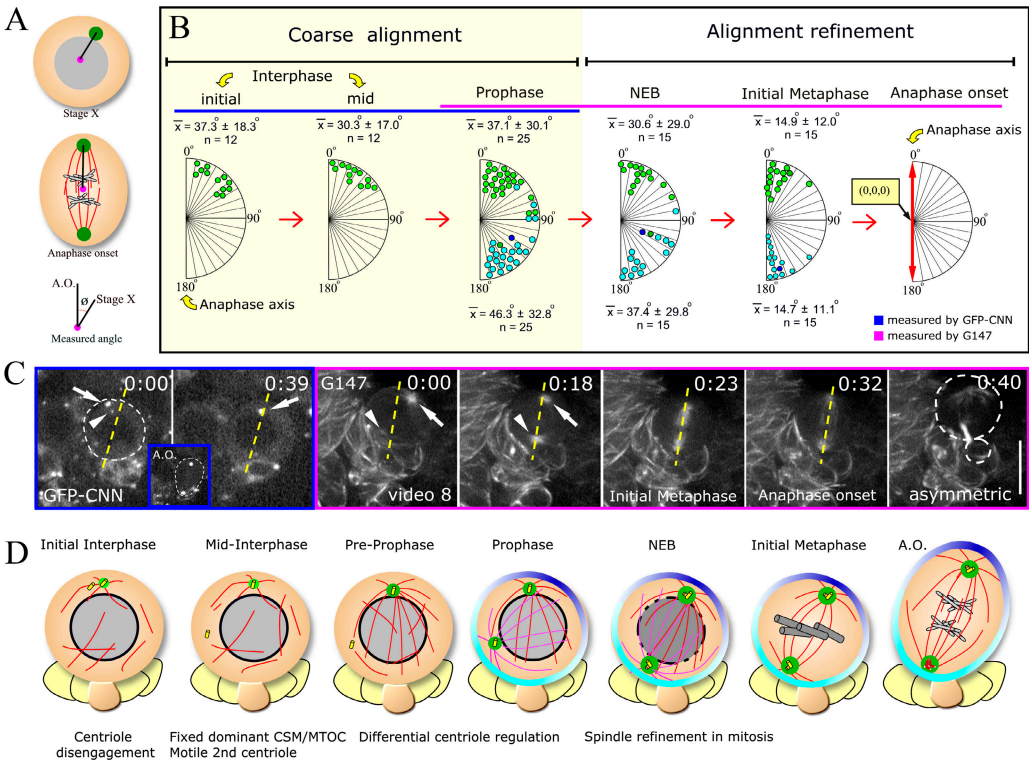

Figure 4. **Two phases of spindle alignment.** (A) Cartoon showing measured angles. (B) Centrosome location relative to anaphase division axis onset. Green circles indicate the dominant centrosome, and blue circles indicate the second centrosome. In 1/25 NBs, the dominant centrosome (dark green) was on the GMC side of the nucleus at prophase; its second centrosome is shown in dark blue. Measurements used Cnn (blue; interphase and prophase) or MTs (pink). (C) Sample video stills. Yellow lines indicate anaphase-onset axis. (D) Cartoon showing centrosome/centriole cycles. Time is shown as h:min. Bar, 10 μm.

Our data suggest that differences exist. It is unlikely that this differential regulation is a result of location, as both centrioles are initially adjacent after disengagement. The differences may be due to centriole age or procentriole maturation state.

The dominant centrosome predicts spindle alignment

The NB spindle is largely aligned by NEB (Siller et al., 2006). Based on our data, we tested the hypothesis that the dominant centrosome helps define one spindle pole before prophase. We calculated the angle between the dominant centrosome/MTOC axis (Fig. 4 A, top) and the anaphase axis (bottom), using the nuclear centroid as a fixed reference. This revealed two phases in defining the future spindle axis. Through prophase onset, the dominant centrosome remains fairly stationary roughly opposite the GMCs (Fig. 4 B, coarse alignment), agreeing with fixed images (Ceron et al., 2001), whereas the second centriole moves to a distal position (to within 46 ± 33° [$n = 25$] of the anaphase axis; Fig. 4 B, prophase). This is consistent with our hypothesis. The dominant centrosome may be immobilized by aster–cortex interactions or by absence of an active displacement mechanism. In the second phase, alignment is refined in prophase and prometaphase (the angle between the NB centrosome and anaphase axes decreases from 31 ± 29° to 15 ± 12°; $n = 15$), as shown by Siller et al. (2006).

To further test whether anchoring the dominant centrosome helps roughly align the spindle, we imaged *asl* mutant NBs live. They lack functional centrosomes (Giansanti et al., 2001; Fig. S3 A, available at http://www.jcb.org/cgi/content/full/jcb.200612140/DC1) and astral MTs. Mutant NBs lack a dominant interphase centrosome, allowing us to assess its role in spindle orientation and asymmetric cell division. Live imaging revealed robust chromatin-mediated MT nucleation and spindle assembly producing fairly normal spindles (Fig. 5 A and Video 9). Spindle poles emerge from a disorganized MT array near the chromosomes that focuses as the spindle lengthened. Spindles do not rotate during formation, always forming along the initial pole separation axis, but do rotate during metaphase (23 ± 15°; $n = 11$), suggesting that rotation can occur without astral MTs or that *asl* mutants have a reduced astral array sufficient for rotation (Fig. 5 A). Surprisingly, consecutive divisions in *asl* mutants usually produce adjacent or near-adjacent daughters ($n = 5/5$; Fig. 5 B and Video 10), as in wild type (Fig. 1 E). In a few cases, however, spindles form parallel to the GMC cap and, presumably, the polarity axis (2/13; ~15%); these NBs divide symmetrically (Fig. 5 C). This suggests that the second phase of spindle alignment can occur without a dominant centrosome and can rescue misalignment, as long as it is not too extreme, but occasional atypical symmetric divisions occur. This results in defective brain anatomy,

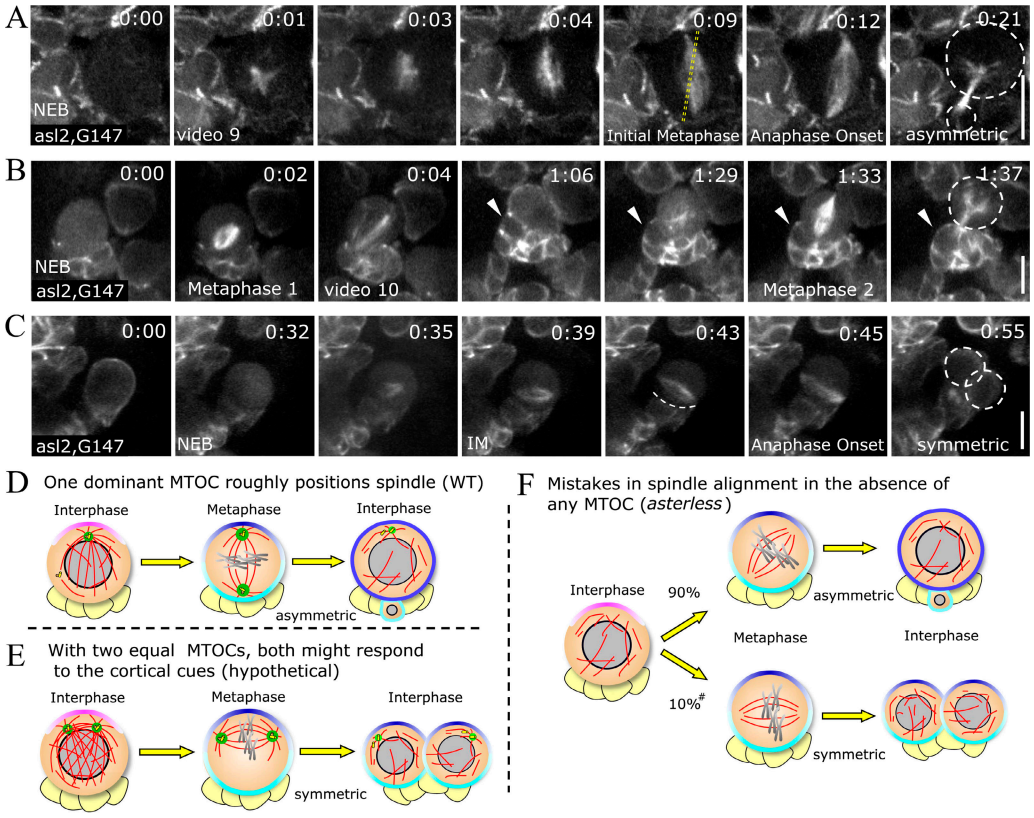

Figure 5. **Functional centrosomes ensure high-fidelity division asymmetry.** (A–C) GFP-G147 in *asl*. (A) Chromosome-induced spindle assembly (0:01–0:09). Initial spindle alignment is absent, but refinement occurs (0:09–0:12). (B) Two rounds of mitosis. GMCs born near one another. Arrowheads indicate first daughter. (C) Example where initial spindle alignment was far off NB-GMC axis, with resulting symmetric division. (D) Mechanistic model of the importance of dominant interphase MTOC. (E) Hypothetical case: centrosomes matured synchronously as in canonical cycle. (F) Division with no centrosomes. Pound sign indicates that number is from fixed analysis of telophase NBs (Giansanti et al., 2001). Time is shown as h:min. Bars, 10 μm.

with ectopic paired, smaller NBs, presumably progeny of symmetric divisions (Fig. S3 B).

A novel centrosome cycle helps ensure fidelity of spindle position

Our data reveal two new aspects of asymmetric division in this stem cell model. First, cells can adjust the canonical centrosome cycle to allow novel cell behaviors, as was observed during clam meiosis (Wu and Palazzo, 1999). Central brain NBs also alter this cycle: rather than both centrosomes maturing in synchrony and proximity (Fig. 5 E), the two centriole pairs are differentially regulated, maturing asynchronously and distant from one another (Fig. 5 D). One retains MT nucleating activity throughout the cell cycle, forming the dominant MTOC during interphase, whereas the second is initially inactive, only forming a functional centrosome and nucleating MTs at mitotic entry. One speculative possibility is that these are mother and daughter centrioles and that one is preferentially retained in the stem cell, a hypothesis that will now be tested. It is also of interest to ask whether other stem cells use this mechanism.

Second, our data suggest that this novel centrosome cycle helps ensure high-fidelity spindle positioning and thus asymmetric division (Fig. 5 D). We propose a model in which NB mitotic spindles are aligned in two phases to ensure that GMC daughters are born next to the previous GMC. Rough alignment is achieved by confining the dominant MTOC to a relatively fixed position from the previous division and moving the second centriole to the other side of the cell. As spindles form, a second process refines this initial alignment. In *asl* mutants, without centrosomes, the first mechanism is inactive, but the second mechanism can align the spindle unless initial alignment is wildly off axis (Fig. 5 F). In *mud* mutants, centriole separation must occur normally, as prophase MTOCs are nearly fully separated, but alignment of spindle poles to cortical polarity cues is defective (Siller et al., 2006). The normal two-step process is a robust mechanism ensuring successful asymmetric divisions and reproducible brain anatomy.

Materials and methods

Fly stocks

y w flies were the wild-type controls for all immunostained samples. For live-cell imaging, we used the following strains: *UAS-actin-GFP* (Jacinto et al., 2000), *UAS-GFP-Cnn1* (Megraw et al., 2002), *GFP-G147* (GFP-tagged MT-associated protein; Morin et al., 2001), *UAS-EB1-GFP* (a gift from S. Rogers [University of North Carolina at Chapel Hill, Chapel Hill, NC] and B. Eaton [University of Texas at San Antonio, San Antonio, TX]), *GFP-PACT* (Martinez-Campos et al., 2004), and *Polo-GFP* (Moutinho-Santos et al., 1999). We generated transgenic flies of the genotype *UAS-mCherry-α-tubulin* and *mCherry-SAS-6* by using a standard P-element transformation (Rubin and Spradling, 1982). mCherry-α-tubulin (human tubulin) was PCR amplified from an unknown expression vector (a gift from A. Straight, Stanford University, Stanford, CA) and cloned into the pUASg vector. mCherry-SAS-6 (generated by G. Rogers, University of North Carolina at Chapel Hill) is expressed under its endogenous promoter and was cloned into the pCaSpeR4 vector. All UAS promoters were driven by Gal4-1407 (Bloomington Drosophila Stock Center). For fixed samples of *asl* mutants, we identified homozygous *asl*^{2} larvae by selecting against the *Tubby* marker on the *TM6* Balancer (Giansanti et al., 2001). For live imaging of MTs in the *asl* background, we generated recombinants of the genotype *asl*^{2}*,G147/TM6*.

Live-cell imaging of NBs in the intact larval brain

Crawling third instar larvae were dissected in Schneider's Drosophila Medium (Invitrogen) with 10% FCS. The entire brain was explanted and placed anterior side down (ventral nerve cord upward) in our imaging chamber (Fig. S1). Brains were allowed to settle in the center of a pool of media in a glass-bottomed dish (MatTek). The media was surrounded by Halocarbon oil 700, which supported a glass coverslip used to seal the chamber. Samples were imaged using a Yokogawa spinning disk confocal (PerkinElmer) mounted on a microscope (Eclipse TE300; Nikon). It is equipped with an interline cooled charge-coupled device camera (ORCA-ER; Hamamatsu), a z-focus motor (Prior Scientific), an excitation and an emission wheel controlled by the Lambda 10-2 controller (Sutter Instrument) and emission filters from Semrock. Objectives used were 100× 1.4 NA, 60× 1.4 NA, and 40× oil 1.3 NA. 4D and 5D (x, y, z, time, wavelength) video sequences were collected using the multidimensional acquisition add-on in MetaMorph (Molecular Devices).

NB immunostaining

Brains of *y w* and *asl*^{2}*/asl*^{2} flies were fixed in 9% formaldehyde or 4% paraformaldehyde in PTA (PBS + 0.1% Tween 20 + 0.2 g/l sodium azide) for 15 min, blocked in 1% normal goat serum for 3 h, and stained in a microcentrifuge tube in primary antibody and 1% normal goat serum in PTA overnight at 4°C. Brains were washed and incubated in secondary antibodies for 2 h at room temperature. The following antibodies were used: E7 mouse anti–α-tubulin (1:250; Developmental Studies Hybridoma Bank), rabbit anti-DPLP (1:1,000; Martinez-Campos et al., 2004), mouse GTU-88 anti–γ-tubulin (1:500; Sigma-Aldrich), and rabbit anti-GFP (1:750; ab290 [Abcam]). Secondary antibodies were Alexa 488 and 546 (Invitrogen) and were used at a final concentration of 1:500.

Measuring angles between the centrosome and the anaphase-onset division axis

For each selected time point, the (x, y, z) coordinates of the centrosome was recorded. We also recorded the coordinates for the point of origin at each time point, which we designated as center of the nucleus from interphase to NEB, the center of the chromosomal mass at initial metaphase, and half the distance between the slightly separated sister chromatids at anaphase onset. At each time point, the origin was normalized to (0, 0, 0) and the centrosome coordinates were adjusted accordingly. This method eliminated the effects of x, y, z stage/microscope drift. The following equation was used to measure the angle between the two defined vectors (x1, y1, z1) and (x2, y2, z2): Dot Product = (x1 × x2) + (y1 × y2) + (z1 × z2) = L1 × L2 × cos(Θ), where L, length of vector, equals the square root of ($x^2 + y^2 + z^2$) and Θ is the angle between the two vectors. Note that all the measured angles are in relation to the anaphase-onset vector, which was always designated as the (x2, y2, z2) vector.

For the interphase time points, we used GFP-Cnn (Fig. 4 B, blue), because the interphase centrosome could not always be identified with high confidence using an MT marker. We used GFP-G147 to stage cells at prophase (appearance of second MTOC), NEB (flood of fluorescence into the nucleus), initial metaphase (judged by spindle shape), and anaphase onset (kinetochore MT shortening; Fig. 4 B, pink).

Online supplemental material

Video 1 shows wild-type NBs expressing actin-GFP through two rounds of mitosis. Video 2 presents a side view of wild-type GFP-G147–expressing NBs during mitotic entry. Video 3 gives an end-on view of wild-type GFP-G147–expressing NBs during mitotic entry. Video 4 shows wild-type NBs expressing GFP-Cnn through an entire cell cycle. Video 5 shows wild-type NB expressing chTub and GFP-Cnn, showing PCM splitting during mitotic exit. Video 6 presents wild-type NB expressing chTub and GFP-PACT. Video 7 shows wild-type NB expressing mCherry-SAS-6 and Polo-GFP during mitotic entry. Video 8 shows wild-type GFP-G147–expressing NBs during mitotic entry and through the end of telophase. Video 9 shows *asl*^{2}*,G147* mutant NBs during spindle assembly and through mitosis. Video 10 shows *asl*^{2}*,G147* mutant NBs through two rounds of mitosis. Fig. S1 provides a sample preparation and MT distribution in NBs. Fig. S2 shows CNN and Polo behavior throughout the cell cycle. Fig. S3 shows that *asl* mutant brains contain supernumerary central brain NBs. Online supplemental material is available at http://www.jcb.org/cgi/content/full/jcb.200612140/DC1.

We thank C. Doe, T. Kaufman, P. Martin, C. Sunkel, M. Gatti, and J. Raff for reagents; S. Rogers and B. Eaton for the unpublished EB1-GFP fly stock; and A. Khodjakov, T. Salmon, K. Bloom, S. Rogers, and G. Rogers for helpful discussions.

N.M. Rusan is supported by American Cancer Society grant PF-06-108-CCG. This work was supported by National Institutes of Health grant GM67236.

Submitted: 22 December 2006
Accepted: 5 March 2007

Note added in proof. While this work was in review, two relevant papers were published. Rebollo et al. (Rebollo, E., P. Sampaio, J. Januschke, S. Llamazares, H. Varmark, and C. Gonzalez. 2007. *Dev. Cell.* 12:467–474) also investigated centrosomes in *Drosophila* neuroblasts, and Yamashita et al. (Yamashita, Y.M., A.P. Mahowald, J.R. Perlin, and M.T. Fuller. 2007. *Science.* 315:518–521) studied centrosomes in another *Drosophila* stem cell model, the male germline stem cells.

References

Akong, K., B.M. McCartney, and M. Peifer. 2002. *Drosophila* APC2 and APC1 have overlapping roles in the larval brain despite their distinct intracellular localizations. *Dev. Biol.* 250:71–90.

Alberts, B., A. Johnson, J. Lewis, M. Raff, K. Roberts, and P. Walter. 2002. Molecular biology of the cell. Garland Science, New York. 1616 pp.

Basto, R., J. Lau, T. Vinogradova, A. Gardiol, C.G. Woods, A. Khodjakov, and J.W. Raff. 2006. Flies without centrioles. *Cell.* 125:1375–1386.

Callaini, G., and M.G. Riparbelli. 1990. Centriole and centrosome cycle in the early *Drosophila* embryo. *J. Cell Sci.* 97:539–543.

Ceron, J., C. Gonzalez, and F.J. Tejedor. 2001. Patterns of cell division and expression of asymmetric cell fate determinants in postembryonic neuroblast lineages of *Drosophila*. *Dev. Biol.* 230:125–138.

Cottam, D.M., J.B. Tucker, M.M. Rogers-Bald, J.B. Mackie, J. Macintyre, J.A. Scarborough, H. Ohkura, and M.J. Milner. 2006. Non-centrosomal microtubule-organising centres in cold-treated cultured *Drosophila* cells. *Cell Motil. Cytoskeleton.* 63:88–100.

Dammermann, A., T. Muller-Reichert, L. Pelletier, B. Habermann, A. Desai, and K. Oegema. 2004. Centriole assembly requires both centriolar and pericentriolar material proteins. *Dev. Cell.* 7:815–829.

Delattre, M., and P. Gonczy. 2004. The arithmetic of centrosome biogenesis. *J. Cell Sci.* 117:1619–1630.

Giansanti, M.G., M. Gatti, and S. Bonaccorsi. 2001. The role of centrosomes and astral microtubules during asymmetric division of *Drosophila* neuroblasts. *Development.* 128:1137–1145.

Glover, D.M. 2005. Polo kinase and progression through M phase in *Drosophila*: a perspective from the spindle poles. *Oncogene.* 24:230–237.

Jacinto, A., W. Wood, T. Balayo, M. Turmaine, A. Martinez-Arias, and P. Martin. 2000. Dynamic actin-based epithelial adhesion and cell matching during *Drosophila* dorsal closure. *Curr. Biol.* 10:1420–1426.

Kellogg, D.R., M. Moritz, and B.M. Alberts. 1994. The centrosome and cellular organization. *Annu. Rev. Biochem.* 63:639–674.

Kuriyama, R., and G.G. Borisy. 1981. Centriole cycle in Chinese hamster ovary cells as determined by whole-mount electron microscopy. *J. Cell Biol.* 91:814–821.

Martinez-Campos, M., R. Basto, J. Baker, M. Kernan, and J.W. Raff. 2004. The *Drosophila* pericentrin-like protein is essential for cilia/flagella function, but appears to be dispensable for mitosis. *J. Cell Biol.* 165:673–683.

Megraw, T.L., L.R. Kao, and T.C. Kaufman. 2001. Zygotic development without functional mitotic centrosomes. *Curr. Biol.* 11:116–120.

Megraw, T.L., S. Kilaru, F.R. Turner, and T.C. Kaufman. 2002. The centrosome is a dynamic structure that ejects PCM flares. *J. Cell Sci.* 115:4707–4718.

Mimori-Kiyosue, Y., N. Shiina, and S. Tsukita. 2000. The dynamic behavior of the APC-binding protein EB1 on the distal ends of microtubules. *Curr. Biol.* 10:865–868.

Morin, X., R. Daneman, M. Zavortink, and W. Chia. 2001. A protein trap strategy to detect GFP-tagged proteins expressed from their endogenous loci in *Drosophila*. *Proc. Natl. Acad. Sci. USA.* 98:15050–15055.

Moutinho-Santos, T., P. Sampaio, I. Amorim, M. Costa, and C.E. Sunkel. 1999. In vivo localisation of the mitotic POLO kinase shows a highly dynamic association with the mitotic apparatus during early embryogenesis in *Drosophila*. *Biol. Cell.* 91:585–596.

Nystul, T.G., and A.C. Spradling. 2006. Breaking out of the mold: diversity within adult stem cells and their niches. *Curr. Opin. Genet. Dev.* 16:463–468.

Piehl, M., U.S. Tulu, P. Wadsworth, and L. Cassimeris. 2004. Centrosome maturation: measurement of microtubule nucleation throughout the cell cycle by using GFP-tagged EB1. *Proc. Natl. Acad. Sci. USA.* 101:1584–1588.

Piel, M., P. Meyer, A. Khodjakov, C.L. Rieder, and M. Bornens. 2000. The respective contributions of the mother and daughter centrioles to centrosome activity and behavior in vertebrate cells. *J. Cell Biol.* 149:317–330.

Rubin, G.M., and A.C. Spradling. 1982. Genetic transformation of *Drosophila* with transposable element vectors. *Science.* 218:348–353.

Savoian, M.S., and C.L. Rieder. 2002. Mitosis in primary cultures of *Drosophila* melanogaster larval neuroblasts. *J. Cell Sci.* 115:3061–3072.

Shaw, S.L., E. Yeh, P. Maddox, E.D. Salmon, and K. Bloom. 1997. Astral microtubule dynamics in yeast: a microtubule-based searching mechanism for spindle orientation and nuclear migration into the bud. *J. Cell Biol.* 139:985–994.

Siller, K.H., M. Serr, R. Steward, T.S. Hays, and C.Q. Doe. 2005. Live imaging of *Drosophila* brain neuroblasts reveals a role for Lis1/dynactin in spindle assembly and mitotic checkpoint control. *Mol. Biol. Cell.* 16:5127–5140.

Siller, K.H., C. Cabernard, and C.Q. Doe. 2006. The NuMA-related Mud protein binds Pins and regulates spindle orientation in *Drosophila* neuroblasts. *Nat. Cell Biol.* 8:594–600.

Wu, X., and R.E. Palazzo. 1999. Differential regulation of maternal vs. paternal centrosomes. *Proc. Natl. Acad. Sci. USA.* 96:1397–1402.

Yamashita, Y.M., D.L. Jones, and M.T. Fuller. 2003. Orientation of asymmetric stem cell division by the APC tumor suppressor and centrosome. *Science.* 301:1547–1550.

Yu, F., C.T. Kuo, and Y.N. Jan. 2006. *Drosophila* neuroblast asymmetric cell division: recent advances and implications for stem cell biology. *Neuron.* 51:13–20.